CHEMISTRY
A European Journal

A Journal of
ChemPubSoc Europe

Accepted Article

Title: The Taming of Redox-Labile Phosphidotitanocene Cations

Authors: Adrien Thomas Normand, Quentin Bonnin, Stéphane Brandès, Philippe Richard, Paul Fleurat-Lessard, Charles Devillers, Cédric Balan, Pierre Le Gendre, Gerald Kehr, and Gerhard Erker

To be cited as: *Chem. Eur. J.* 10.1002/chem.201805430

Link to VoR: http://dx.doi.org/10.1002/chem.201805430

Supported by
ACES

WILEY-VCH

10.1002/chem.201805430

WILEY-VCH

FULL PAPER

The Taming of Redox-Labile Phosphidotitanocene Cations

Adrien T. Normand,[a]* Quentin Bonnin,[a] Stéphane Brandès,[a] Philippe Richard,[a] Paul Fleurat-Lessard,[a] Charles H. Devillers,[a] Cédric Balan,[a] Pierre Le Gendre,[a]* Gerald Kehr[b] and Gerhard Erker[b]

Abstract: d^0 phosphidotitanocene cations stabilized with a pendant tertiary phosphane arm are reported. These compounds were obtained by one-electron oxidation of d^1 precursors with $[Cp_2Fe][BPh_4]$. The electronic structure of these compounds was studied experimentally (EPR, UV-vis and NMR spectroscopy, X-ray diffraction analysis) and through DFT calculations. The theoretical analysis of the bonding situation using the Electron Localization Function (ELF) shows the presence of π interactions between the phosphido ligand and Ti in the d^0 complexes, whereas dπ-pπ repulsion prevents such interactions in the d^1 complexes. In addition, CH/π interactions were observed in several complexes, both in solution and in the solid state, between the phosphido ligand and the phosphane arm. The d^0 complexes were found to be light sensitive, and decompose via Ti-P bond homolysis to give Ti(III) species. A naked d^0 phosphidotitanocene cation has been trapped by reaction with diphenylacetylene, yielding a Ti / P frustrated Lewis pair (FLP) which was found to be less reactive than a previously reported Zr analogue.

Introduction

Group 4 metal complexes bearing anionic phosphorus ligands have been investigated since the mid-1960s.[1] Numerous studies focused on the reactivity and catalytic applications of Zr phosphinidene (**A**) and Zr phosphido (**B**) complexes (Scheme 1, R_2P^-: phosphido; RP^{2-}: phosphinidene).[2],[3] By contrast, the corresponding Ti complexes have been somewhat less explored; initially, most reports dealt with the synthesis and characterization of Ti phosphido complexes (**B'**) ─ including P-bridged bimetallic compounds ─ with little emphasis on reactivity.[4] Later reports by Harrod, Stephan and Le Gendre highlighted the importance of Ti phosphido species in catalytic dehydrocoupling and hydrophosphination reactions.[5] Finally, Ti phosphinidene complexes (**A'**) have been studied by Mindiola.[6]

[a] Dr. A. T. Normand, Dr Q. Bonnin, Dr S. Brandes, Dr P. Richard, Dr C. H. Devillers, C. Balan, Prof P. Le Gendre
ICMUB, Université de Bourgogne Franche-Comté, UFR sciences et techniques, 9 rue Alain Savary - BP 47870, 21078 Dijon Cedex (France).
E-mail: adrien.normand@u-bourgogne.fr; pierre.le-gendre@u-bourgogne.fr
[b] Dr G. Kehr, Prof.G. Erker
Organisch-Chemisches Institut, Universität Münster
Corrensstrasse 40, 48149 Münster (Germany)

Supporting information for this article is given via a link at the end of the document. CCDC 1871408-1871418 contain the supplementary crystallographic data for this paper. These data can be obtained free of charge from the Cambridge Crystallographic Data Centre via www.ccdc.cam.ac.uk/datarequest/cif.

We have recently reported on the chemistry of d^0 phosphidozirconocene cations (**C**).[7] Compared to neutral complexes, these species display enhanced reactivity due to the combination of a coordinatively unsaturated Cp_2Zr^{2+} fragment with a nucleophilic PR_2^- ligand. This reactivity can be exploited in *i)* the cooperative activation of CO_2 and organic substrates; *ii)* the catalytic hydrogenation of olefins; *iii)* the synthesis of Zr^+ / P frustrated Lewis pairs (FLPs) by cycloaddition with alkynes. Unfortunately, we have thus far been unable to isolate these species and conduct more detailed investigations into the nature of the Zr-P bond.

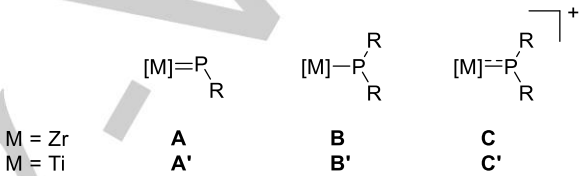

Scheme 1. Group 4 metal complexes with anionic phosphorus ligands.

In parallel to these studies, we have also been exploring the possibility to generate phosphidotitanocene cations (**C'**). Compared to the Zr analogues, these compounds require a different synthetic approach. Indeed, the salt metathesis route employed with Zr is unfeasible with Ti, since Ti(IV) compounds are prone to one-electron reduction with concomitant production of a phosphinyl radical.[9]

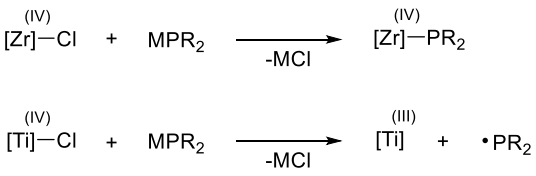

Scheme 2. Reaction of group 4 metals with alkali metal phosphides (M = Li, Na, K).[10]

As a consequence, examples of isolable Ti(IV) phosphido complexes are rather rare,[3a-b],[11] and to the best of our knowledge, experimentally characterized examples of d^0 phosphidotitanocene complexes are unknown. However, we surmised that stable d^0 phosphidotitanocene cations might be obtained by oxidation of readily available neutral Ti(III) precursors containing a pendant phosphine arm (Scheme 3).[12]

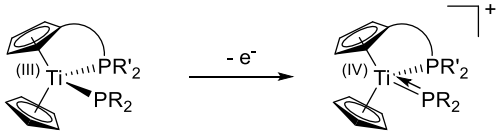

Scheme 3. Synthesis of d^0 phosphidotitanocene cations by one-electron oxidation of neutral Ti(III) precursors.

In this paper, we report the successful application of this strategy and we address the question of the nature of the Ti-P bond in **C'** both experimentally and theoretically (DFT). Finally, we compare the reactivity of a FLP derived from an unsubstituted phosphidotitanocene cation with that of its previously reported Zr counterpart.

Results and Discussion

The synthesis of the target phosphidotitanocene cations can be effected in two steps from previously described [$Cp^PCpTiCl_2$] complexes **1**.[13] Ti(III) precursors were first prepared on 1-2 mmol scale by reacting 2 eq of lithium phosphide (PPh_2Li or PCy_2Li) with **1** (Scheme 4).[14]

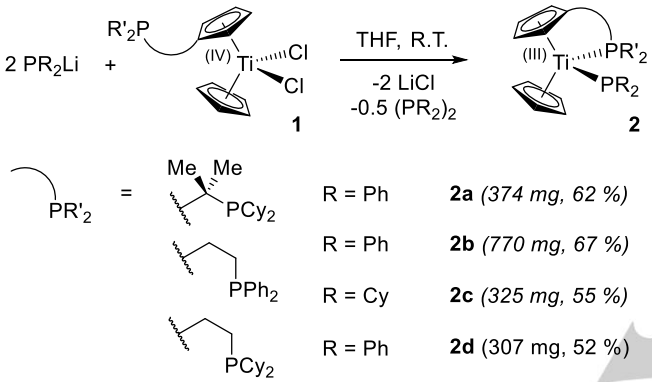

Scheme 4. Synthesis of neutral Ti(III) precursors **2a-d**.

Compounds **2a-d** were obtained as green (**2a**, **2b**, **2d**) or brown (**2c**) solids in moderate yield. They were characterized by EPR spectroscopy, UV-vis spectroscopy, X-ray diffraction and elemental analysis.

Unlike the $TiCl_2$ precursors **1a-d**, compounds **2a-d** all show an interaction between Ti and the pendant phosphine arm in the solid state (Figure 2). Table 1 provides a summary of relevant metric parameters; data for the analogous compound [$Cp_2Ti(PPh_2)(PMe_3]$ (**D**) previously reported by Stephan are also included for comparison.[4j]

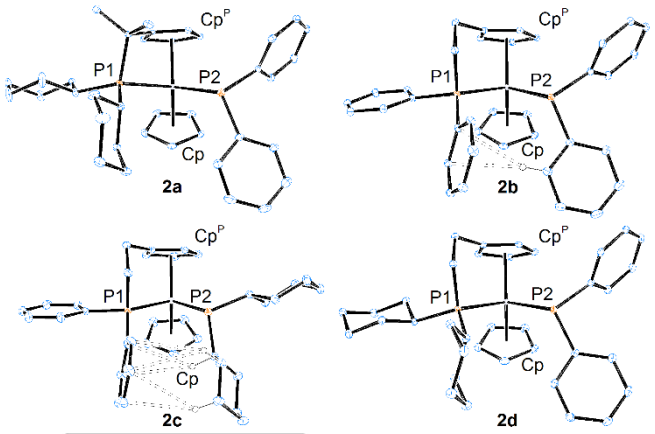

Figure 1. ORTEP drawings of the X-ray structures of **2a-d** (ellipsoids drawn at the 30% probability level, hydrogen atoms removed for clarity, except where CH-π interactions are highlighted).

Table 1. Relevant bond lengths [Å] and angles [°] for **2a-d**.[a]

	2a	2b	2c	2d	D[b]
Ti-Cp^P	2.0556(12)	2.0713(8)	2.0802(9)	2.0804(11)	2.088(5)[c]
Ti-Cp	2.0528(14)	2.0527(9)	2.0612(9)	2.0617(12)	2.074(4)
Ti-P1[d]	2.6652(8)	2.5990(6)	2.6040(5)	2.6499(8)	2.636(3)
Ti-P2[d]	2.6636(8)	2.6641(5)	2.6247(6)	2.6600(8)	2.658(3)
Cp-Ti-Cp^P	137.40(5)	135.99(3)	135.24(4)	134.44(4)	133.18(19)
P1-Ti-P2	93.40(2)	85.33(2)	79.76(2)	86.02(2)	86.02(9)
Σα(P2)	319.6(2)	322.5 (1)	333.8(1)	325.3(2)	324.5(5)

[a] Cp and Cp^P indicate the centroid of the Cp and Cp^P rings, respectively; [b] literature values; [c] Ti-Cp distance; [d] P1: phosphane ligand, P2: phosphido ligand.

The most salient structural feature of complexes **2a-d** and **D** is the pseudo tetrahedral geometry of the phosphido ligand. This is reflected in the sum of angles around P1, with values ranging from 319.6(2)° (**2a**) to 333.8(1)° (**2c**). Electronic repulsion between the phosphorus lone pair and the singly-occupied 1a1 orbital of the d^1 metal centre is most likely responsible for this geometry,[2d],[15] which should entail a trigonal planar phosphido ligand for the oxidized complexes (*vide infra*). The absence of π-interactions between the phosphorus lone pair and the Cp_2Ti fragment is also evident from *i*) the orientation of the phosphido ligand,[16] and *ii*) the relatively long Ti-P2 distances (from 2.6247(6), **2c**, to 2.6641(5), **2b**) which are close to the sum of covalent radii of Ti and P (2.67±0.11Å).[17] These experimental findings are corroborated by theoretical calculations conducted on **2b** (vide infra).

It is interesting to compare the structures of **2b** and **2c**, since the latter features the considerably more basic and bulkier PCy_2^- (compared to PPh_2^-) phosphido ligand. First of all, the Ti-P2 distance in **2c** is 0.039 Å shorter compared to **2b**; the phosphido ligand is also somewhat flatter in **2c**, with a larger sum of angles around P2 (+11.3 °). It is tempting to ascribe these observations to increased π-interactions between Ti and PCy_2^-, but the orientation of PCy_2^- is not adequate for this purpose. A closer inspection of the structure of **2c** suggests another explanation, namely CH/π interactions.[18] Indeed, according to Nishio's formalism, **2c** contains two Cy hydrogens in region 2 above one of the Ph rings of the phosphane arm, and one in region 1 (see the Supporting Information): therefore, these hydrogens satisfy the criteria for CH/π interactions.[19] As a consequence, the Cy ring is brought closer to the phosphane arm, with concomitant flattening of the phosphido ligand, and shortening of the Ti-P2 distance. The narrower P1-Ti-P2 angle in **2c** (79.76(2)°) compared to **2b** (85.33(2)°) is also likely a consequence of these interactions. Noteworthy, **2b** also features a hydrogen atom in region 1 above one of the phosphane arm's Ph ring, however this is achieved simply by orienting both Ph rings in a perpendicular fashion.

10.1002/chem.201805430

The X-band EPR spectra of **2a-d** were recorded in THF and toluene at 295 K. Due to the extreme moisture sensitivity of these compounds, hydrolysis products were generally observed in increasing amounts over time. The EPR spectrum of **2b** in toluene shown in Figure 2 illustrates this phenomenon (see the supporting information for a detailed discussion).

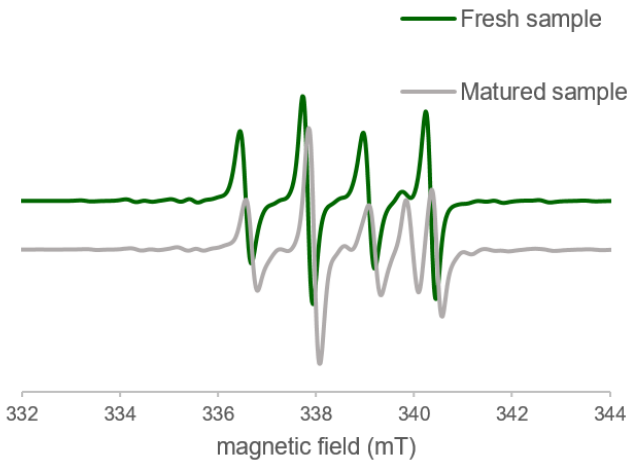

Figure 2. EPR spectrum of **2b** in toluene showing the apparition of a hydrolysis product over time.

Relevant parameters (isotropic g-factor, hyperfine and superhyperfine coupling constants) are gathered in Table 2, along with data for **D** previously reported by Stephan.[4j] Theoretical values were obtained by DFT calculations (see the Supporting Information for details).

Table 2. Relevant EPR parameters for **2a-d**.[a]

	2a	**2b**	**2c**	**2d**	**D**[b]
g	1.9885	1.9911	1.9922	1.9895	-
	1.9885	1.9912	1.9922	1.9896	1.991
Calc.[c]	*1.9865*	*1.9884*	*1.9896*	*1.9856*	*1.988*
$A^{47/49Ti}$	9.0	8.7	8.3	9.1	-
	9.0	8.7	8.5	9.0	8.6
Calc.[c]	*6.2*	*5.9*	*5.8*	*6.2*	*4.2*
A^{31P}-1	21.0	23.3	22.7	22.4	-
	21.3	23.3	22.3	22.3	24.4
Calc.[c]	*-20.9*	*-19.9*	*-19.1*	*-17.7*	*-29.8*
A^{31P}-2	6.3	11.0	16.3	4.8	-
	8	12.0	17.3	5.3	2.1
Calc.[c]	*9.9*	*15.4*	*15.7*	*10.5*	*-6.3*

[a] spectra recorded in THF (first line) or toluene (second line) at 295 K; a values in 10^{-4}.cm^{-1} [b] literature values, spectrum recorded in toluene at 298 K.[c] Computed in toluene.

Remarkably, the values of g and A for each compound are very similar in THF and toluene, which implies that phosphane coordination is retained in THF. This behaviour is also observed with the d^0 phosphidotitanocene cations (*vide infra*).

The absolute values of the coupling constant to the phosphido ligand (A^{31P}-2) range from 4.8 to 16.3.10^{-4} cm^{-1} in THF. These are consistently smaller than the values of the coupling constant to the phosphane arm (A^{31P}-1), which span a much more restricted range of 21.0 to 22.7.10^{-4} cm^{-1}. These values are consistent with those found by Stephan for **D**,[4j] and they are a consequence of the higher s character of the Ti-phosphane bond. Indeed, NBO calculations indicate ~40 % s character for the latter, *vs* ~20 % for the Ti-phosphido bond (see the Supporting Information).

The UV-vis absorption spectra of **2a-d** in THF are characterized by local maxima (ε= 570-1410 cm^{-1}.M^{-1}) in the red to near IR region (Figure 3).[20]

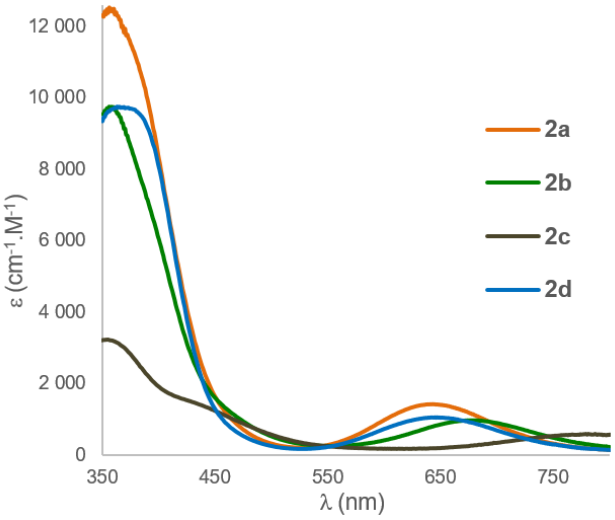

Figure 3. UV-vis spectra of **2a-d** in THF.

As TD-DFT is not reliable for open-shell systems,[21] we were unable to confidently analyse these transitions theoretically, and can therefore only speculate as to their exact nature.

We next turned our attention to the synthesis of the target phosphidotitanocene cations **3**, following the oxidation route described above (Scheme 3). Thus, Ti(III) complexes **2a-d** were oxidized with $[Cp_2Fe][BPh_4]$ in C_6H_5Br, following a modification of a previously reported procedure.[13b]

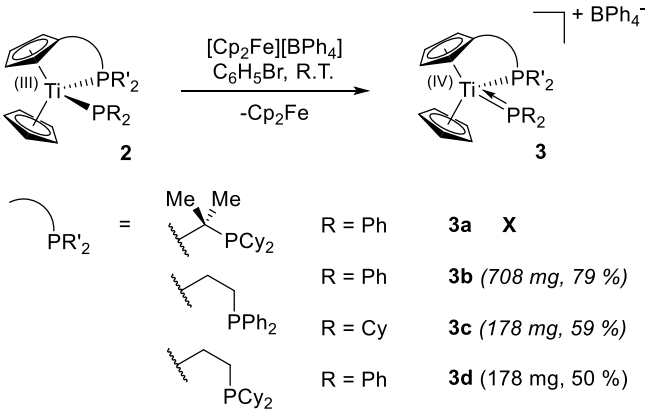

Scheme 5. Synthesis of phosphidotitanocene cations **3b-d**.

Complexes **3b-d** were isolated in good to moderate yield after workup (Scheme 5); however, complex **3a** could not be isolated

in pure form (the Cp region of the ^{1}H NMR spectrum showed the presence of impurities, and the mixture could not be purified).

We also attempted the synthesis of the unsubstituted phosphidotitanocene complex $[Cp_2Ti(PCy_2)][BPh_4]$ (**3e**) following the oxidation route described in Scheme 4. Addition of two equivalents of PCy_2Li to $[Cp_2TiCl_2]$ in C_6H_5Br followed by oxidation with $[Cp_2Fe][BPh_4]$ led to a mixture of dia- and paramagnetic species, possibly including the $[Cp_2Ti(PCy_2)(PCy_2H)]^+$ cation (see the Supporting Information). When we repeated this experiment in THF, the known compound $[Cp_2Ti(THF)_2][BPh_4]$ was isolated as blue crystals in 23 % overall yield after recrystallization (Scheme 6).[22] This complex was most probably formed by homolysis of the Ti-P bond according to Scheme 2.

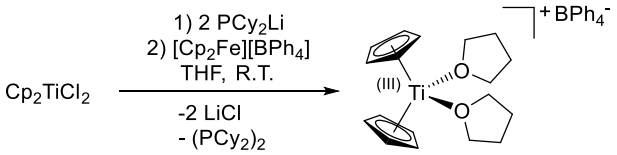

Scheme 6. Attempted syntheses of an unsubstituted d^0 phosphidotitanocene cation.

In light of the difficulties associated with the oxidation route, we attempted a different approach involving the protonolysis of the Cp_2TiMe^+ cation with PCy_2H (Scheme 7). Interestingly, this route did not afford **3e**, but instead compound **3f**, which contains a coordinated PCy_2H ligand. Attempts at preparing **3e** by using only 1 eq of PCy_2H failed; rather, mixtures of **3f** and Cp_2TiMe^+ were obtained. A PPh_2 analogue (**3g**) could also be synthesized, using PPh_2H instead of PCy_2H.

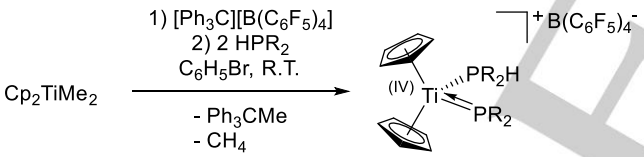

R = Cy **3f** *(1.20 g, 83 %)*
R = Ph **3g** *(0.98 g, 83 %)*

Scheme 7. Synthesis of d^0 phosphidotitanocene cations stabilized by secondary phosphanes.

Altogether, these results suggest that mixed phosphane / phosphidotitanocene cations are quite stable. Indeed, not only could complexes **3b-f** be isolated and studied spectroscopically (NMR, EPR, UV-vis), but X-ray structures were also obtained for **3b**, **3c** and **3e** (Figure 4).

The impact of oxidation is evident upon examination of the solid-state structures of complexes **2b** / **3b** and **2c** /**3c** (Tables 1 and 3). The Ti-P2 distance is 0.30 Å shorter in **3b** *vs* **2b**, and 0.26 Å shorter in **3c** *vs* **2c**. Additionally, the phosphido ligand in complexes **3** is now much closer to a trigonal planar geometry than in complexes **2**, thus bringing the phosphorus lone pair closer to Ti (Σα(P2) = 358.9(3) to 360.0(4)°). Moreover, the orientation of the phosphido ligand (torsion angle φ) also brings the lone pair into the same plane as the empty 1a1, b2 and 2a1 orbitals on Ti.[23] The unconstrained PPh_2H complex **3e** is a case in point, with a Ti-P2 bond distance of 2.3611(18) Å (much shorter than the 2.67±0.11Å sum of covalent radii), a perfectly trigonal planar phosphido ligand (Σα(P2) = 360.0(4)°) and an almost perfect alignment of donor-acceptor orbitals (φ = -2.3(3) °). These changes are especially remarkable if one considers that other parameters (*e.g.* Ti-P1 distances), hardly change upon oxidation.

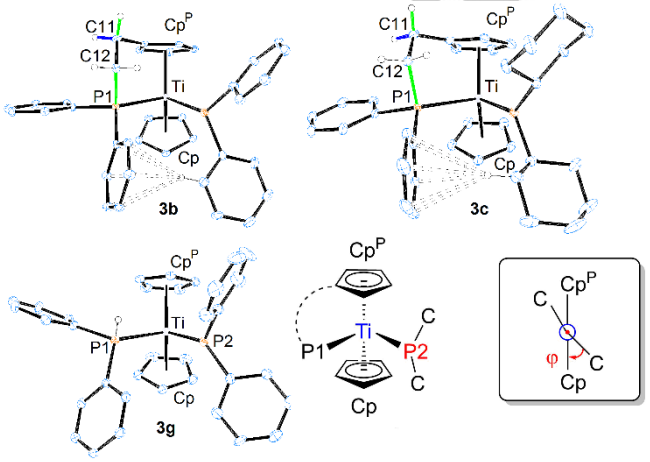

Figure 4. ORTEP drawings of the X-ray structures of **3b-g** (ellipsoids drawn at the 30% probability level, BPh_4^- anion and most hydrogen atoms removed for clarity) and definition of the torsion angle φ.

Table 3. Relevant bond lengths [Å] and angles [°] for **3b, 3c and 3e**.[a]

	3b	**3c**	**3e**
Ti-Cp^P	2.0471(18)	2.0497(9)	2.051(3)[c]
Ti-Cp	2.040(3)	2.0438(9)	2.042(3)
Ti-P1[d]	2.5883(12)	2.6062(5)	2.5868(17)
Ti-P2[d]	2.3599(14)	2.3646(6)	2.3611(18)
Cp-Ti-Cp^P	135.20(9)	133.77(4)	134.89(12)
P1-Ti-P2	90.72(4)	89.26(2)	88.83(6)
Σα(P2)	358.9 (3)	359.98(12)	360.0(4)
φ	16.09(19)	-15.85(8)	-2.3(3)

[a] Cp and Cp^P indicate the centroid of the Cp and Cp^P rings, respectively; [b] literature values; [c] Ti-Cp distance; [d] P1: phosphane ligand, P2: phosphido ligand.

Therefore, there is considerable structural evidence to support the hypothesis of π interactions between Ti and the phosphido ligand in complexes **3**. This is confirmed through the theoretical analysis of the Ti-P interactions in **2b** and **3b** (see Computational Details): in **2b**, only one lone pair of the phosphido ligand is involved in a Ti-P bond, while both are interacting with the titanium atom in **3b** (Figure 5) indicating π interactions in these complexes.[24] This is in line with previous theoretical results obtained on hypothetical d^0 phosphidotitanocene complexes.[12]

A deeper analysis of the X-ray structures of **3b** and **3c** reveals yet more interesting features. Firstly, as in the case of **2b** and **2c**, CH/π interactions are observed between one of the Ph rings of

10.1002/chem.201805430

the phosphane arm and CH bonds on the phosphido ligand (Figure 4). Both hydrogens are located in region 1 above the Ph rings (see the Supporting Information). Interestingly, in the case of **3c**, this does not seem to induce a narrower P1-Ti-P2 angle as in **2c**. Rather, since the Cy ring is engaged in only one CH/π interaction with the Ph ring, both rings adopt a perpendicular orientation, as observed with the Ph rings of **2b** and **3b**.

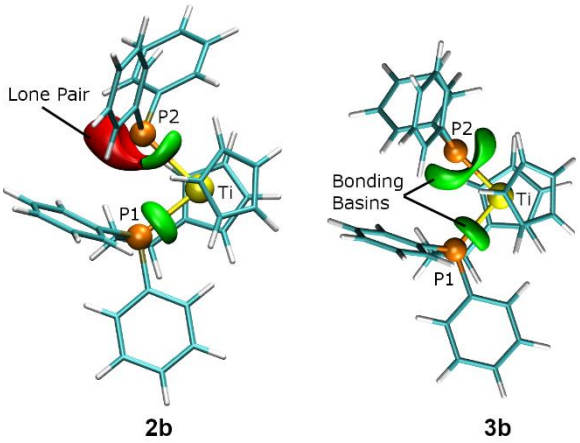

Figure 5. ELF basins in **2b** and **3b**. Bonding basin are shown in green whilst lone pairs are in red. For clarity's sake, only the basins between Ti and P are shown, and the BPh_4^- anion is omitted.

Secondly, the chelate ring formed by the phosphane arm causes one of the CH bonds of the CH_2 group attached to the Cp ring to become almost anti-periplanar to the P1-CH_2 bond (Figure 6).

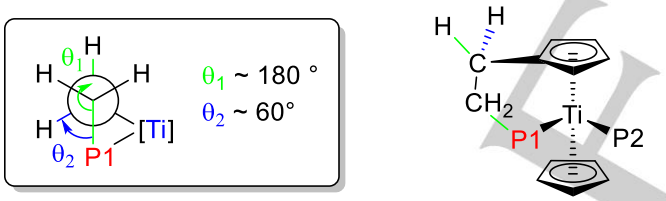

Figure 6. Definition of torsion angles θ_1 and θ_2.

Examination of the ^{1}H NMR spectrum of **3b** and **3c** indicates that this conformation is retained in solution. Indeed, Figure 7 shows the aliphatic region of the ^{1}H and ^{1}H{^{31}P} spectra of **3b**: the hydrogens of the Cp-CH_2 group resonate at 2.87 and 2.04 ppm, with $^3J_{PH}$ coupling constants of 44.9 and 5.5 Hz (Table 4).[25] Since ^3J coupling between P and H nuclei follows a Karplus relationship, with a maximum corresponding to anti-periplanar arrangement of P-C and C-H bonds,[26] we conclude that the conformation of the ethylene arm of **3b** is similar in solution and in the solid state.[27] The same conclusions can also be drawn for **3c**.

The CH/π interactions observed in the X-ray structures of **3b** and **3c** should entail considerably shielded ^{1}H NMR signals for the hydrogens involved, due to aromatic ring current effects. Indeed, in the case of **3b**, the *ortho* hydrogens of one of the Ph ring of the phosphido ligand resonate as a triplet at 6.25 ppm in CD_2Cl_2 (500 MHz, 300 K), whereas the same hydrogens resonate above 7.28 ppm in **3d** (Figure 8).[28] However, CH-π interactions are not strong enough to prevent the free rotation of the Ph ring of the phosphido ligand.

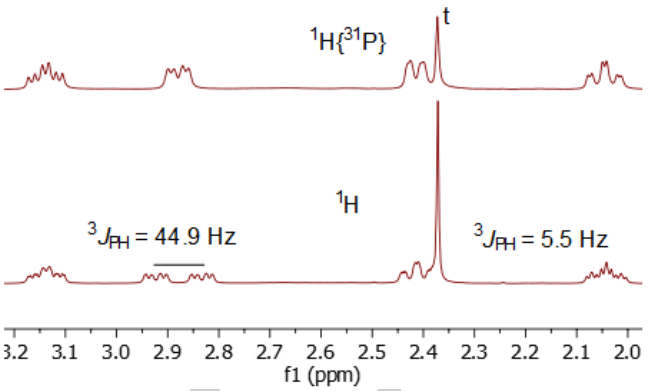

Figure 7. Aliphatic region of the ^{1}H and ^{1}H{^{31}P} spectra of **3b** in CD_2Cl_2 (500 MHz, 300 K) showing ^3J coupling between P and H nuclei (t: residual toluene signal).

Table 4. Values of θ (XRD) and $^3J_{PH}$ (NMR) for **3b** and **3c** .[a]

	θ_1 (°)	θ_2 (°)	$^3J_{PH}$-1 (Hz)	$^3J_{PH}$-2 (Hz)
3b	172.1(3)	-69.5(4)	44.9	5.5
3c	-174.66(12)	67.08(16)	43.5	6.1

[a] ^{1}H spectra recorded at 500 MHz in CD_2Cl_2, 300 K.

In the case of **3c**, a shielded signal (0.00 ppm) is observed in CD_2Cl_2 (500 MHz, 300 K) for one of the CH_2 hydrogens of the Cy ring. Interestingly, a shielded signal is also observed in d_8-THF (0.06 ppm) and C_6D_5Br (-0.17 ppm). The conformation of this complex appears to be frozen in these solvents at 300 K, since only one hydrogen experiences a shielding effect (probably because of steric congestion due to the Cy ring).

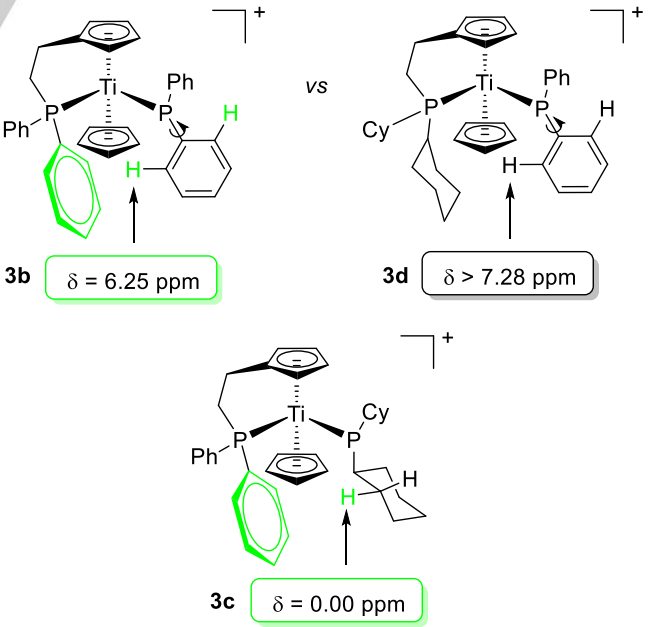

Figure 8. Conformational origin of shielded ^{1}H NMR signals in **3b** and **3c** (CD_2Cl_2, 500 MHz, 300 K). BPh_4^- anions omitted for clarity.

10.1002/chem.201805430

In summary, there is considerable evidence to suggest that the structures of **3b** and **3c** are the same in solution and in the solid state. This correspondence indicates that the Cp^PCpTi fragment (Cp^P = C_5H_5-$CH_2CH_2PPh_2$) may be viewed as a pre-organized host for CH/π interactions with incoming ligands or substrates. Noteworthy, the neutral d^1 analogues are also pre-organized, since the X-ray structures of **2b** and **2c** show CH/π interactions as well.

The $^{31}P\{^1H\}$ NMR spectra of **3b-g** are also interesting in a number of ways. First of all, the signals corresponding to the phosphido ligand are very deshielded, around 410 ppm for PPh_2^- and 500 ppm for PCy_2^- (Table 5). For comparison, the $[Cp_2ZrPCy_2]^+$ cation (**C1)** gave a more shielded signal at 396.6 ppm (C_6D_5Br, 202 MHz, 299 K).[7a] In a recent paper, Eisenstein noted that neutral d^0 alkylidene complexes — which are valence isoelectronic to cationic d^0 phosphido complexes — display considerably deshielded ^{13}C NMR signals, similar to carbocations, despite their nucleophilic carbene character.[29] The major conclusion of that study was that the observed deshielding of the carbene signal (compared to ethylene) was the result of more efficient coupling between σ_{MC} (ligand based) and π^*_{MC} (metal based) orbitals, which are separated by a narrower gap than the σ_{CC} and π^*_{CC} orbitals of ethylene. Consequently, d^0 alkylidene complexes of 5d metals give less deshielded carbene signals than isoelectronic 4d metals complexes, due to the higher energy of 5d *vs* 4d empty orbitals. Although this would fall outside the scope of the present paper, it would be interesting — in light of the Eisenstein study — to investigate whether similar explanations apply to *i)* the highly deshielded ^{31}P NMR signal of phosphidometallocene cations **3b-f** and **C1**, and *ii)* the ~100 ppm difference between Ti (3d) and Zr (4d) complexes.

Table 5. Relevant $^{31}P\{^1H\}$ NMR parameters for **3b-g**.[a]

	3b	3c	3d	3g	3f
δ-P1[b]	45.2	43.8	52.3	23.7	39.1
(ppm)	44.9	43.2	52.2	N.A.[c]	N.A.[c]
δ-P2	414.1	506.4	401.2	420.2[c]	500.4[c]
(ppm)	408.8	496.7	395.1	N.A.[d]	N.A.[d]
$^2J_{PP}$	70.2	71.7	64.0	83.0	76.7
(Hz)	68.7	70.6	63.0	N.A.[c]	N.A.[c]

[a] spectra recorded in CD_2Cl_2 (first line) or d_8-THF (second line) at 202 MHz, 300 K; [b] P1: phosphane ligand, P2: phosphido ligand; [c] spectra recorded in C_6D_5Br; [d] **3e** and **3f** decomposed in THF.

Another striking feature of complexes **3b-f**, visible in their $^{31}P\{^1H\}$ spectra, is the stability conferred by the chelating phosphane arm in a coordinating solvent such as d_8-THF. Indeed, complexes **3b-d** remain unaltered in this solvent, as evidenced by the similar chemical shifts of P1 and P2 in CD_2Cl_2 *vs* d_8-THF on the one hand, and the $^2J_{PP}$ coupling constants on the other hand (64.0 to 71.7 Hz in CD_2Cl_2 *vs* 63.0 to 70.6 Hz in d_8-THF). In contrast, dissolution of **3e** or **3f** in d_8-THF releases free PPh_2H or PCy_2H (see the Supporting Information).

We measured the UV-vis absorption spectra of **3b-d** in THF (Figure 9), and we observed intense bands (ε = 6920-7910 $cm^{-1}.M^{-1}$) in the blue region (**3b** -> 437nm; **3c** -> 419 nm; **3d** -> 448 nm).

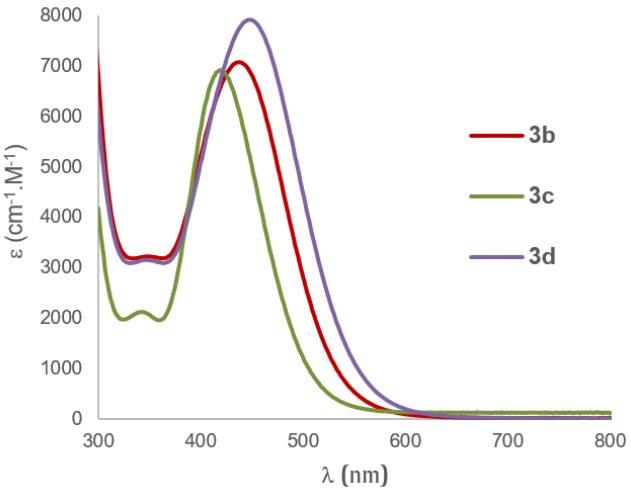

Figure 9. UV-vis spectra of **3b-d** in THF.

DFT calculations were conducted to investigate the nature of this transition. Natural Transition Orbitals (Figure 10) indicate that it corresponds to a LMCT band, mostly centred on the phosphido ligand.[30]

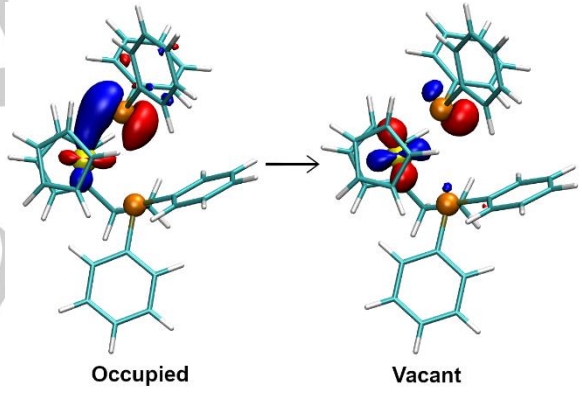

Figure 10. Natural Transition Orbitals for the highest energy UV-vis band of **3b**.

Since d^0 phosphidotitanocene are usually unstable and readily decompose to give Ti(III) and phosphinyl radicals (Scheme 2), we were intrigued by the apparent stability of complexes **3b-g**. The presence of π interactions between the Cp_2Ti fragment and the phosphido ligand alone cannot explain this stability, as illustrated by our failure to prepare complex **3e**. We reasoned that the additional phosphane ligand in **3b-g** might simply provide kinetic stabilization to otherwise thermodynamically unstable entities. To test this hypothesis, we measured the EPR spectra of **3b-g** and found that paramagnetic Ti-P species were present in every case. In the case of **3f** and **3g**, we could positively identify the $Cp_2Ti(THF)_2^+$ cation as the main paramagnetic species (g = 1.9758, $A^{47/49Ti}$ = 11.4 x 10^{-4} cm^{-1}). For complexes **3b-d**, the spectra revealed the presence of at least three paramagnetic Ti-P species (see the Supporting Information).

Irradiation of **3g** and **3g** with a UV lamp for 20 minutes led to mixtures in which only the $Cp_2Ti(THF)_2^+$ cation was visible by EPR spectroscopy (Figure 11).

10.1002/chem.201805430

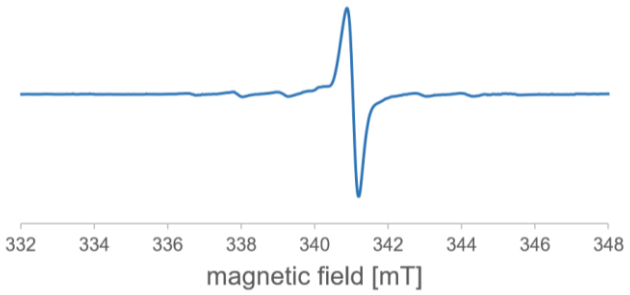

Figure 11. EPR spectrum of **3g** after 20 min irradiation with a UV lamp

Analysis of the reaction mixtures by $^{31}P\{^{1}H\}$ and $^{11}B\{^{1}H\}$ NMR spectroscopy revealed *i)* the complete disappearance of **3f** and **3g**, *ii)* an intact $B(C_6F_5)_4^-$ anion, *iii)* concomitant formation of $(PPh_2)_2$ for **3g**, and *iv)* the apparition of several P-containing species in addition to PCy_2H for **3f** (some of which was present before irradiation).[31]

For complexes **3b-d**, the mixtures after UV irradiation were again complex by EPR spectroscopy, but in each case the BPh_4^- anion was also intact, whilst the presence of $(PPh_2)_2$ (**3b**, **3d**) or $(PCy_2)_2$ (**3c**) strongly suggested that $PR_2^{\bullet}$ radicals had been generated.

Therefore, it appears that d^0-phosphidotitanocene cations decompose by Ti-P bond homolysis just like their neutral counterparts. Compared to the unsubstituted complex **3e**, the additional stabilization provided by the phosphane ligand in **3b-g** enables the isolation of these otherwise fleeting species.

In light of these findings, we decided to investigate whether complex **3e** could be generated *in situ* and trapped with a suitable reagent. We had previously shown that the Zr analogue of **3e** (**C1**) reacted with diphenylacetylene to give a Zr^+ / P frustrated Lewis pair (FLP),[7a] therefore we generated **3e** in the presence of this reagent, and indeed complex **4e** was isolated in 27 % yield after workup (Scheme 8).

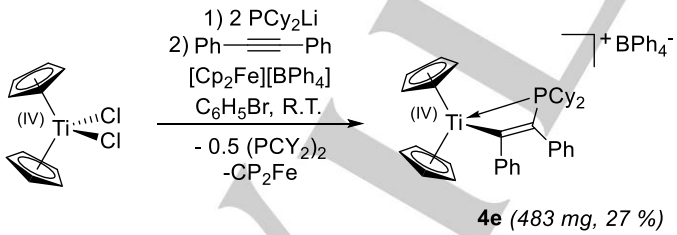

Scheme 8. Synthesis of a Ti^+ / P FLP by the trapping of a phosphidotitanocene cation.

Evidence for the formation of **4e** initially came from the comparison of its ^{1}H and $^{31}P\{^{1}H\}$ NMR spectra with those of the previously reported Zr analogue **E** (containing the $MeB(C_6F_5)_3^-$ anion).[7a] For example, the Cp hydrogens in **4e** resonate as a doublet at 6.52 ppm ($^{3}J_{PH}$ = 1.7 Hz) in CD_2Cl_2, indicative of phosphane coordination to Ti, whilst the $^{31}P\{^{1}H\}$ spectrum shows a signal at -7.6 ppm. Similar spectroscopic features were observed for compound **E** (Cp: 6.23 ppm, $^{3}J_{PH}$ = 0.7 Hz; phosphane : -12.4 ppm).[32]

Interestingly, the high-resolution ESI mass spectrum of **4e** shows the expected presence of the $Cp_2Ti(C(Ph)C(Ph)PCy_2^+$ cation (with a distinctive cluster of peaks at 553.24758 Da), but the elusive $Cp_2Ti(PCy)_2^+$ is also observed (375.17211 Da). This suggests some degree of reversibility for the alkyne insertion reaction, at least under the relatively forcing conditions of the mass spectrometry experiment.

A PPh_2 analogue of **4e** was also prepared by reacting **3e** with a four-fold excess of diphenylacetylene. Although the insertion reaction was much slower (72 h *vs* a few minutes), probably due to the necessity to dissociate PPh_2H first, compound **4e** (not shown) was isolated in 88 % yield. The preparation of **4e** starting from an isolated phosphidotitanocene cation indicates that alkyne insertion probably occurs after oxidation by $[Cp_2Fe][BPh_4]$ during the synthesis of **4e**.

Although **4e** is stable enough to be isolated and characterized by NMR spectroscopy, UV-vis spectroscopy, ESI-MS and X-ray diffraction analysis (*vide infra*), it displays slightly broadened signals by ^{1}H NMR spectroscopy, suggesting the presence of paramagnetic impurities. Indeed, the EPR spectrum of a solution of **4e** in d_8-THF indicated the presence of small amounts of $[Cp_2Ti(THF)_2][BPh_4]$ (see the Supporting Information), which again points to the reversible insertion of diphenylacetylene into the Ti-P bond of **3e**.

Irradiation of this solution with a UV lamp and monitoring the reaction by EPR spectroscopy revealed that a new Ti-P product was being formed in equimolar quantities with $[Cp_2Ti(THF)_2][BPh_4]$. Both ^{1}H and $^{31}P\{^{1}H\}$ spectra showed the complete disappearance of **4e**, although the $^{11}B\{^{1}H\}$ NMR spectrum did not evolve during photolysis. Borates are known to decompose photolytically in the presence of electron acceptors,[33] therefore we initially envisaged a non-innocent role for the BPh_4^- anion. However, we could not find any evidence for the oxidation of BPh_4^-, nor could we identify the diamagnetic by-products of the reaction.

The reaction was repeated on preparative scale, and complex **4e'** was isolated in 40 % yield after workup (Scheme 9).

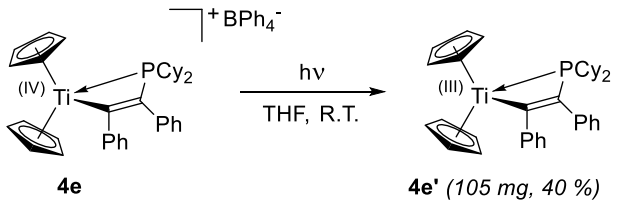

Scheme 9. Synthesis of **4e** by photolysis of **4e**.

Complexes **4e** and **4e'** were characterized by single crystal X-ray diffraction analysis (Figure 12, Table 5). The metric parameters of these complexes support their formulation as Ti-alkenyl complexes with a chelating phosphane arm, rather than Ti-carbene complexes bound to an alkylidene phosphonium moiety.[34] The C11-C12 bond distances are consistent with a double bond (**4e**: 1.344(2) Å; **4e'**: 1.341(4) Å), whilst Ti-C11 and C12-P distances indicate the presence of single bonds (**4e**: 2.178(2) Å and 1.813(2) Å; **4e'**: 2.229(2) Å and 1.798(2) Å). The

10.1002/chem.201805430

shorter Ti-P distance in **4e** reflects the higher Lewis acidity of Ti(IV) vs Ti(III) (**4e**: 2.6421(8) Å; **4e'**: 2.7000(8) Å).

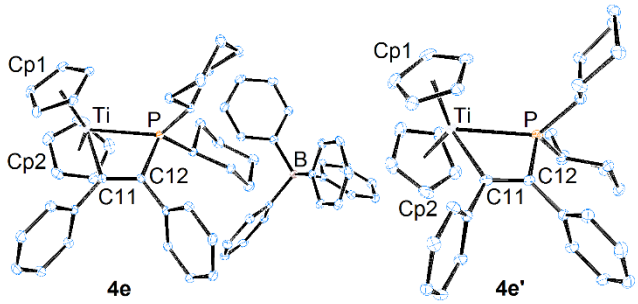

Figure 12. ORTEP drawings of the X-ray structures of **4e** and **4e'** (ellipsoids drawn at the 30% probability level, hydrogen atoms removed for clarity) Cp1 and Cp2 indicate the centroid of the Cp rings. Selected bond distances (Å) and angles (°). **4e:** Ti-Cp1 = 2.0347(9); Ti-Cp2 = 2.0379(9); Ti-P = 2.6421(8); Ti-C11 = 2.178(2); C11-C12 = 1.344(2); C12-P = 1.813(2); Cp1-Ti-Cp2 = 133.83(4); P-Ti-C11 = 63.37(4); Σα(C11) = 359.8(2); Σα(C12) = 359.7(2). **4e':** Ti-Cp1 = 2.0562(13); Ti-Cp2 = 2.0623(13); Ti-P = 2.7000(8); Ti-C11 = 2.229(2); C11-C12 = 1.341(4); C12-P = 1.798(2); Cp1-Ti-Cp2 = 133.46(6); P-Ti-C11 = 61.22(6); Σα(C11) = 359.6(3); Σα(C12) = 359.9(3).

In order to determine the redox properties of the **4e/4e'**, couple, voltammetric analyses were performed in THF, with 0.1 M $NaBPh_4$ as electrolyte. Under these conditions, **4e** is reversibly reduced at $E_{1/2}$ = −0.420 V *vs.* SCE (Figure 13). The reduced species was attributed to the Ti(III) complex **4e'**. Complementary cyclic and steady state voltammetry experiments conducted on a mixture of **4e** and **4e'** confirmed that these compounds form one redox couple, and can be reversibly transformed into each other (see the supporting information).

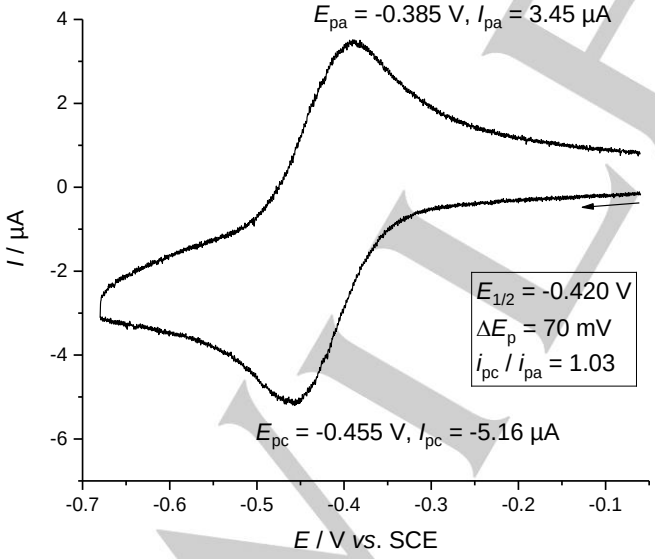

Figure 13. **4e** in THF 0.1 M $NaBPh_4$ ([**4e**] = 5 x 10^{-4} M, v = 100 mV s^{-1}, working electrode: GC electrode Ø = 3 mm, counter electrode: Pt, Reference electrode: SCE).

Finally, we investigated the FLP behaviour of **4e**. By contrast with the Zr analogue **E**, reaction with chalcone or 1 atm CO_2 at room temperature in CD_2Cl_2 did not yield the expected FLP adducts: no reaction was observed in both cases. However, when **4e** was reacted with ferrocene carboxaldehyde in CH_2Cl_2, compound **5e** was obtained in 83 % yield after workup (Scheme 10).

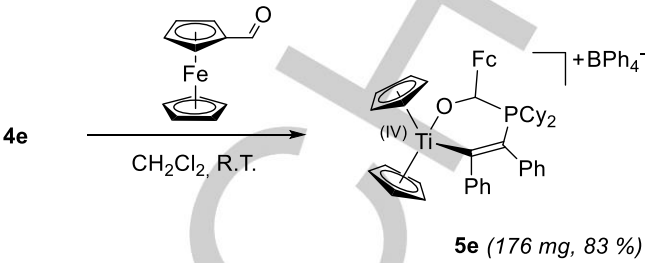

Scheme 10. FLP reaction of **4e** with ferrocene carboxaldehyde.

Compound **5e** exhibits characteristic NMR features in CD_2Cl_2, indicative of the activation of the CHO moiety by the Ti /P FLP. Firstly, the $^{31}P\{^1H\}$ NMR spectrum shows a signal at 32.5 ppm (**4e**: -7.6 ppm), consistent with the presence of a phosphonium moiety. Secondly, the activated aldehydic proton resonates as a broad signal at 6.12 ppm in the ^1H spectrum, and couples both with the carbons of the ferrocene Cp ring and the CH carbons of the Cy rings in the HMBC spectrum. Finally, the activated aldehydic carbon resonates as a doublet at 80.2 ppm ($^1J_{PC}$ = 49.2 Hz) in the $^{13}C\{^1H\}$ spectrum.

The high resolution ESI spectrum of **5e** displays a single cluster of peaks at 767.25649 Da, which is again consistent with FLP adduct formation.

Single crystals suitable for X-ray diffraction were obtained by slow diffusion of pentane into a CH_2Cl_2 solution of **5e** at -18 °C (Figure 14).

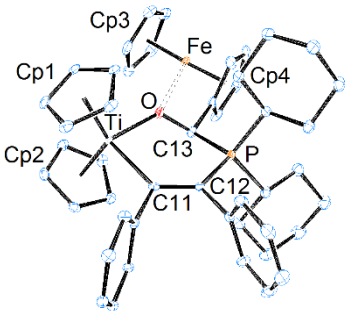

Figure 14. ORTEP drawings of the X-ray structure of **5e** (ellipsoids drawn at the 30% probability level, hydrogen atoms, BPh_4^- anion and CH_2Cl_2 solvate molecules removed for clarity).

Compared to **4e**, the Ti-C11 distance (2.231(3) Å) is significantly elongated (+0.053(4) Å). The C11-C12 distance is somewhat elongated (1.361(3) Å, +0.017(4) Å), whilst the C12-P distance is slightly shortened (1.800(3) Å, -0.013(4) Å). Noteworthy, the Fe-O distance (3.521(2) Å) is shorter than the sum of Van der Waals radii (3.94 Å), a feature which was previously observed in a related Zr complex.[35]

Finally, complex **4e'** failed to react with ferrocene carboxaldehyde (toluene, room temperature), highlighting the

greater Lewis acidity of the d^0 titanocenium cation compared to its neutral d^1 sibling.

Conclusions

Although d^0 phosphidotitanocene complexes are intrinsically unstable due to their redox-labile nature, we have shown that they can be isolated as phosphane-stabilized cations. This is somewhat counter-intuitive, since d^0 complexes are classified as hard Lewis acids, whilst phosphorus-based ligands fall in the category of soft Lewis bases. It appears that the phosphane-stabilized phosphidotitanocene cations reported in this study are unique in many ways: although they are stable enough to be isolated and crystallographically characterized, they readily decompose in the presence of light. Additionally, they have strikingly similar structures in solution and in the solid state, a consequence of the pre-organization of the phosphane-functionalized metallocenium fragment in a favourable conformation for CH/π interactions. Thus, in contrast to their redox-labile behaviour, they show great structural resilience even in coordinating solvents such as d_8-THF. Finally, they give rise to extremely high ^{31}P NMR chemical shifts, in the 400-500 ppm range, as a consequence of the double-bond character of the Ti-P interaction.

Experimental Section

General

General information, detailed reaction procedures, analytical details, and structural data of the new compounds are given in the Supporting Information.

Synthesis

Compound 2a: In an Ar glovebox, a solution of PPh_2Li (408 mg, 2.0 mmol) in THF (6 mL) was added to a suspension of complex **1a** (487 mg, 1.0 mmol) in THF (8 mL). The reaction mixture turned green almost instantly, and was stirred at room temperature for 30 min. Volatiles were removed *in vacuo* outside the glovebox, and toluene (15 mL) was added to the residue. The resulting suspension was filtered over diatomaceous earth to remove LiCl, and the filtrate was evaporated. The residue was taken inside the glovebox, and Et_2O (15 mL) was added, forming a green precipitate. It was filtered over a sintered glass frit, rinsed with 3x10 mL of Et_2O, then 2x10 mL of pentane, then dried on the frit, yielding **2a** as a green microcrystalline solid (374 mg, 62 %).
Single crystals suitable for X-ray diffraction analysis were obtained by slow diffusion of pentane into a toluene solution of **2a** at -18°C. Elemental Analysis: calcd for $C_{37}H_{47}P_2Ti$: C, 73.87; H, 7.87. Found: C, 73.17; H, 7.71.

Compound 2b: A solution of PPh_2Li (769 mg, 4.0 mmol) in THF (40 mL) was added to a solution of complex **1b** (920 mg, 2.0 mmol) in THF (40 mL). The reaction mixture turned green almost instantly, volatiles were removed *in vacuo*, and toluene (30 mL) was added to the residue. The resulting suspension was filtered over diatomaceous earth to remove LiCl, and the filtrate was evaporated. The residue was taken inside the glovebox, and a mixture of Et_2O (25 mL) and pentane (25 mL) was added, forming a green precipitate. It was filtered over a sintered glass frit, rinsed with 3x4 mL of a 1:1 mixture of Et_2O/pentane, then dried on the frit, yielding **2b** as a green powder (770 mg, 67 %). Single crystals suitable for X-ray diffraction analysis were obtained by slow diffusion of pentane into a toluene solution of **2b** at -18°C. Elemental Analysis: a satisfactory elemental analysis could not be obtained for this compound despite repeated attempts (C content was always low by 5-10 %).

Compound 2c: In an Ar glovebox, a solution of PCy_2Li (408 mg, 2.0 mmol) in THF (6 mL) was added to a solution of complex **1c** (461 mg, 1.0 mmol) in THF (6 mL). The reaction mixture turned brown almost instantly, volatiles were removed *in vacuo* outside the glovebox, and toluene (30 mL) was added to the residue. The resulting suspension was taken back inside the glovebox, filtered over diatomaceous earth to remove LiCl, and the filtrate was evaporated outside the glovebox. The residue was taken inside the glovebox and triturated in Et_2O (20 mL), forming a brown precipitate. It was filtered over a sintered glass frit, rinsed with 3x4 mL of a 1:1 mixture of Et_2O/pentane, then dried on the frit, yielding **2c** as a brown powder (325 mg, 55 %). Single crystals suitable for X-ray diffraction analysis were obtained by slow diffusion of pentane into a toluene solution of **2c** at -18°C. Elemental Analysis: calcd for $C_{36}H_{45}P_2Ti$: C, 73.59; H, 7.72. Found: C, 73.40; H, 7.60.

Compound 2d: In an Ar glovebox, a solution of PCy_2Li (408 mg, 2.0 mmol) in THF (6 mL) was added to a solution of complex **1c** (461 mg, 1.0 mmol) in THF (6 mL). The reaction mixture turned green almost instantly, volatiles were removed *in vacuo* outside the glovebox, and toluene (30 mL) was added to the residue. The resulting suspension was taken back inside the glovebox, filtered over diatomaceous earth to remove LiCl, and the filtrate was evaporated outside the glovebox. The residue was taken inside the glovebox and triturated in Et_2O (20 mL), forming a green precipitate. It was filtered over a sintered glass frit, rinsed with 3x4 mL of a 1:1 mixture of Et_2O/pentane, then dried on the frit, yielding **2d** as a brown powder (307 mg, 52 %). Single crystals suitable for X-ray diffraction analysis were obtained by slow diffusion of pentane into a toluene solution of **2d** at -18°C. Elemental Analysis: calcd for $C_{36}H_{45}P_2Ti$: C, 73.59; H, 7.72. Found: C, 73.34; H, 7.59.

Compound 3b: In an Ar glovebox, **2b** (574 mg, 1.0 mmol) and $[Cp_2Fe][BPh_4]$ (505 mg, 1.0 mmol) were mixed in C_6H_5Br (5 mL). The reaction mixture gradually turned from green to red over 5 min; residual particles of $[Cp_2Fe][BPh_4]$ were observed. After decantation, the supernatant was added to 50 mL of pentane under vigorous agitation. A brick-red solid formed, it was filtered over a sintered glass frit, suspended three times in pentane (5 mL) and dried on the frit. The resulting powder was freed from residual C_6H_5Br and $[Cp_2Fe]$ by dissolution in CH_2Cl_2 (4 mL), filtration over diatomaceous earth, and precipitation as previously. Finally, the obtained product was stirred in toluene (8 mL) for 3h, then filtered and rinsed with toluene and pentane, yielding **3b** as a brick-red powder containing 50 mol% of toluene and 15 mol% of pentane (708 mg, 79 %). Single crystals suitable for X-ray diffraction analysis were obtained by slow diffusion of pentane into a CH_2Cl_2 solution of **3b** at -18°C. Elemental Analysis: calcd for $C_{60}H_{53}BP_2Ti(C_7H_8)_{0.5}(C_5H_{12})_{0.15}$: C, 81.10; H, 6.23. Found: C, 79.88; H, 6.04.

Compound 3c: In an Ar glovebox, **2c** (196 mg, 0.33 mmol) and $[Cp_2Fe][BPh_4]$ (168 mg, 0 mmol) were mixed in C_6H_5Br (5 mL). The reaction mixture gradually turned from green to red over 5 min; residual particles of $[Cp_2Fe][BPh_4]$ were observed, hence the mixture was filtered over diatomaceous earth. The resulting solution was added to 100 mL of pentane under vigorous agitation. An orange solid formed, it was filtered over a sintered glass frit, suspended three times in pentane (5 mL) and dried on the frit. The resulting powder was freed from residual C_6H_5Br and Cp_2Fe by stirring in toluene (20 mL). An oil formed initially, which turned into a powder over 10 min. The solid was filtered over a sintered glass frit, suspended three times in toluene (4 mL) then three times in pentane (4 mL) and dried on the fritt. Complex **3c** was obtained as an orange powder containing 66 mol% of toluene (178 mg, 59 %). Single crystals suitable for X-ray diffraction analysis were obtained by slow diffusion of pentane into a CH_2Cl_2 solution of **3c** at -18°C. Elemental Analysis: calcd for $C_{60}H_{64}BP_2Ti(C_7H_8)_{0.66}$: C, 80.30; H, 7.22. Found: C, 79.40; H, 7.17.

Compound 3d: In an Ar glovebox, **2d** (218 mg, 0.37 mmol) and $[Cp_2Fe][BPh_4]$ (188 mg, 0.37 mmol) were mixed in C_6H_5Br (3 mL). The reaction mixture gradually turned from green to red over 5 min;

residual particles of $[Cp_2Fe][BPh_4]$ were observed, hence the mixture was filtered over diatomaceous earth. The resulting solution was added to 100 mL of pentane under vigorous agitation. A brick-red solid formed, it was filtered over a sintered glass frit, suspended three times in pentane (10 mL) and dried on the frit. The resulting powder was freed from residual C_6H_5Br and Cp_2Fe by stirring in toluene (10 mL). An oil formed, the supernatant was discarded, fresh toluene (10 mL) was added and agitation was resumed. A powder formed over a few hours. The solid was filtered over a sintered glass frit, suspended three times in toluene (6 mL) then three times in pentane (10 mL) and dried on the frit. Complex **3d** (178 mg, 50 %) was obtained as an orange powder.. Elemental Analysis: $C_{60}H_{64}BP_2Ti$: C, 79.56; H, 7.12. Found: C, 78.11; H, 7.32.

Attempted synthesis of 3e: In an Ar glovebox, Cp_2TiCl_2 (49.8 mg, 0.2 mmol) and PCy_2Li (81.6 mg, 0.4 mmol) were mixed in C_6H_5Br (2 mL). The mixture turned chocolate brown over 5 min. It was filtered over diatomaceous earth, then $[Cp_2Fe][BPh_4]$ (101 mg, 0.2 mmol) was added and the resulting mixture was stirred for 5 min, during which it turned progressively red. It was filtered over diatomaceous earth in order to remove a green-black insoluble solid. The homogeneous red filtrate was added to 80 mL of pentane under vigorous agitation, to precipitate an orange solid. The precipitate was filtered over a sintered glass frit, suspended three times in pentane (10 mL) and dried on the frit. An orange powder (30 mg) was isolated and analyzed by NMR and EPR spectroscopy.
The ^1H and $^{31}P\{^1H\}$ NMR spectrum suggested the presence of the $Cp_2Ti(PCy_2)(PCy_2H)^+$ cation (compare with **3f**) but impurities were also observed. Moreover the ^1H spectrum showed considerably broadened signals, consistent with the presence of paramagnetic impurities. The EPR spectrum revealed a mixture of species.

Compound 3f: In an Ar glovebox, Cp_2TiMe_2 (200 mg, 0.96 mmol) and $Ph_3CB(C_6F_5)_4$ (888 mg, 0.96 mmol, 1 eq) were mixed for 5 min in 2 mL of C_6H_5Br at room temperature. A solution of PCy_2H (401 mg, 2.02 mmol) in C_6H_5Br was added dropwise to the reaction mixture. The resulting deep-red solution was stirred for 3h until a red precipitate was formed. The suspension was added dropwise to 8 mL of pentane under vigorous agitation to complete the precipitation of the desired red compound. The supernatant was removed and the red precipitate was washed twice with 5 mL of pentane. After removal of traces of pentane *in vacuo*, the red precipitate was dissolved in CH_2Cl_2 and precipitated from pentane as described above (*N.B.: compound **3f** slowly decomposes in CH_2Cl_2, therefore this step must be performed quickly*). Removal of volatiles *in vacuo* yielded complex **3f** (1.20 g, 83 %) as a red powder containing 50 mol% of pentane. Elemental Analysis: calcd for $C_{58}H_{55}BF_{20}P_2Ti(C_5H_{12})_{0.5}$: C, 56.39; H, 4.77; Found: C, 57.00; H, 5.00.

Compound 3g: In an Ar glovebox, Cp_2TiMe_2 (200 mg, 0.96 mmol) and $[Ph_3C][B(C_6F_5)_4]$ (888 mg, 0.96 mmol, 1 eq) were mixed for 5 min in 2 mL of C_6H_5Br at room temperature. A solution of PPh_2H (376 mg, 2.02 mmol) in C_6H_5Br was added dropwise to the reaction mixture. The resulting deep-red solution was stirred for 3h until a red precipitate was formed. The suspension was added dropwise to 8 mL of pentane under vigorous agitation to complete the precipitation of the desired red compound. The supernatant was removed and the red precipitate was washed twice with 5 mL of pentane. After removal of traces of pentane *in vacuo*, the red precipitate was dissolved in CH_2Cl_2 and precipitated from pentane as described above (*N.B.: compound **3g** slowly decomposes in CH_2Cl_2, therefore this step must be performed quickly*). Removal of volatiles *in vacuo* yielded complex **3g** (980 mg, 83 %) as a red powder. Single crystals suitable for X-ray diffraction analysis were obtained by slow diffusion of heptane in a bromobenzene solution of the compound at -18°C. Elemental Analysis: calcd for $C_{58}H_{31}BF_{20}P_2Ti$: C, 57.07; H, 2.45; Found: C, 56.71; H, 2.54.

Compound $[Cp_2Ti(THF)_2][BPh_4]$: In an Ar glovebox, Cp_2TiCl_2 (249 mg, 1.0 mmol) and PCy_2Li (408 mg, 2.0 mmol) were mixed in toluene (5 mL). After 5 min, the brown reaction mixture was filtered through diatomaceous earth and the filtrate was evaporated *in vacuo* outside of the glovebox. The residue was dissolved in THF (10 mL) in the glovebox, and $[Cp_2Fe][BPh_4]$ (485 mg, 0.9 mmol) was added. A blue precipitate appeared gradually; the presence of $(PCy_2)_2$ was ascertained by performing no lock $^{31}P\{^1H\}$ NMR experiment. After 1H reaction, the reaction mixture was filtered over a sintered glass frit, the precipitate was suspended twice in THF (1.5 mL) and twice in pentane (3.0 mL) and dried on the frit. Complex $[Cp_2Ti(THF)_2][BPh_4]$ was obtained as a blue-green powder (327 mg, 51 %). Material suitable for elemental analysis was obtained by diffusion of pentane into a THF solution (50 mL) of the crude product. Royal blue crystals of $[Cp_2Ti(THF)_2][BPh_4]$ were obtained (152 mg, 45 %). Single crystals suitable for X-ray diffraction analysis were obtained by cooling a saturated solution of **$[Cp_2Ti(THF)_2][BPh_4]$** in THF at -18°C. Elemental Analysis: calcd for $C_{36}H_{42}PTi$: C, 78.64; H, 7.23. Found: C, 77.45; H, 7.11.

Compound 4e: In an Ar glovebox, Cp_2TiCl_2 (498 mg, 2.0 mmol) and PCy_2Li (816 mg, 4.0 mmol) were mixed in C_6H_5Br (8 mL). After 5 min, the brown reaction mixture was filtered through diatomaceous earth onto a mixture of $[Cp_2Fe][BPh_4]$ (1.01 mg, 2.0 mmol) and diphenylacetylene (356 mg, 2.0 mmol). A green-brown solution was obtained after 5 min, which was added to 120 mL of pentane under vigorous agitation. A green solid formed, it was filtered over a sintered glass frit, suspended three times in pentane (10 mL) and dried on the frit. The resulting powder was freed from residual C_6H_5Br and Cp_2Fe by dissolution in CH_2Cl_2 (6 mL) and filtration over diatomaceous earth. A blue-green solid was removed, and the resulting homogeneous solution was evaporated to dryness. Toluene (100 mL) was added to the residue, and a green solid formed. The suspension was stirred for 3 h, then filtered over a sintered glass frit. The solid was suspended three times in toluene (15 mL) and three times in pentane (15 mL), and dried on the frit. Complex **4e** was obtained as an olive green powder containing 40 mol% of toluene (483 mg, 27 %). *Complex **4e** slowly degrades over time to give **4e'** (vide infra), which explains the impossibility to obtain a satisfactory elemental analysis despite repeated attempts on different batches.* Single crystals suitable for X-ray diffraction analysis were obtained by slow diffusion of pentane into a CH_2Cl_2 solution of **4e** at -18°C.

Compound 4e': A solution of **4e** (440 mg, 0.48 mmol) in THF (15 mL) was irradiated for 4h30 with a 150 W UV lamp (Heraeus TQ 150). Volatiles were removed *in vacuo* and the residue was stirred in 20 mL of pentane inside an Ar glovebox for several hours. The resulting suspension was filtered on a sintered glass frit, yielding a blue-green solid and a brown solution. The solution was evaporated to dryness, yielding **4e'** as a brown gum (105 mg, 40 %). Single crystals suitable for X-ray diffraction analysis were obtained by cooling a saturated solution of **4e'** in pentane at -18°C. Elemental Analysis: calcd for $C_{36}H_{42}PTi$: C, 78.11; H, 7.65. Found: C, 77.27; H, 8.15.

Compound 4g: In an Ar glovebox, compound **3g** (400 mg, 0.32 mmol) was dissolved in C_6H_5Br (3 mL) with an excess of diphenylacetylene (232 mg, 1.3 mmol) at room temperature and stirred for 72 h. The evolution of the reaction was followed by $^{31}P\{^1H\}$ no lock NMR experiments. The starting red solution became green. The compound was precipitated by addition to 6 mL of pentane under vigorous agitation. An oil formed, the supernatant was discarded and the oil extracted twice with pentane. The black-green residue was dissolved in 2 mL of dichloromethane and precipitated as described above. Compound **4g** was obtained as a light brown powder containing 30 mol% of pentane after drying *in vacuo* (350 mg, 88 %). Elemental Analysis: calcd for $C_{60}H_{30}BF_{20}PTi(C_5H_{12})_{0.3}$: C, 59.47; H, 2.73; Found: C, 59.73; H, 2.44.

Compound 5e: In an Ar glovebox, compound **4e** (170 mg, 0.19 mmol) and ferrocene carboxaldehyde (42 mg, 0.20 mmol) were mixed in CH_2Cl_2 (3 mL). After 5 min, the red reaction mixture was added to 50 mL of pentane under vigorous agitation. A red precipitate formed, which was filtered over a sintered glass frit, rinsed with pentane and dried under vacuum. Compoung **5e** was obtained as a brown-red solid (176 mg, 83 %) containing 75 mol% of pentane Single crystals suitable for X-ray diffraction analysis were obtained by slow diffusion of pentane into a CH_2Cl_2 solution of **5e** at -18°C. Elemental Analysis:

calcd for $C_{71}H_{72}BFeOPTi(C_5H_{12})_{0.75}$: C, 78.69; H, 7.16; Found: C, 77.88; H, 6.74.

Hydrolysis of Ti(III)-PPh_2 complexes

In an Ar glovebox, the Ti(III)-PPh_2 complexes (**2a**: 0.5 mmol; **2b**: 0.19 mmol) were dissolved in 4 mL of THF and treated with 0.5 eq of distilled water in THF. The solution turned blue-violet immediately. The volatiles were removed *in vacuo*, the solid residue was triturated with pentane, filtered and rinsed with pentane. Blue violet powders were obtained in both cases after drying *in vacuo* (**2a**: 60 mg; 2b: **46** mg). EPR spectra of **2a** and **2b** were also recorded in "wet", unstabilized THF (degassed by free-pump-thaw) for comparison purposes.

UV irradiation of Ti(IV) complexes

The $Ti^{(IV)}$ complexes (**3b, 4e**: 0.05 mmol; **3c-g**: 0.01 mmol) were dissolved in THF or d_8-THF and irradiated in sequences of 20 min with a medium pressure Hg lamp (Heraeus TQ 150).

FLP reactions

Compound **4e** (43.6 mg, 0.05 mmol) was dissolved in CD_2Cl_2. Chalcone (10.4 mg, 0.05 mmol) was added and ^1H and $^{31}P\{^1H\}$ NMR spectra were recorded, showing only the presence of both reagents.

Compound **4e** (43.6 mg, 0.05 mmol) was dissolved in CD_2Cl_2 and placed in a Schlenk vessel. The vessel was quickly evacuated, and refilled with 1 atm of CO_2. The reaction mixture was stirred for 2 h, and ^1H and $^{31}P\{^1H\}$ NMR spectra were recorded, showing only the presence of **4e**.

Compound **4e'** (55.4 mg, 0.1 mmol) was dissolved in toluene. Ferrocene carboxaldehyde (21.4 mg, 0.1 mmol) was added and an EPR spectrum was recorded, showing only the presence of **4e'**.

Computational details

All DFT and TD-DFT calculations were carried out with the Gaussian09 code,[36] tightening self-consistent field convergence thresholds (10^{-10} a.u.). Geometries were optimized using the B3PW91 functional, with the def2-TZVP basis set for the titanium and the 6-31+G(d,p) basis set for other atoms.[37] Vertical excitations were computed with TD-DFT using the B3PW91 functional, with the def2-TZVP basis set for the titanium and the 6-311++G(d,p) basis set for other atoms. For each complex, 8 states were considered. The solvent effects of THF were included according to the Polarizable Continuum Model (PCM).[38] All orbital isosurfaces have been plotted with the VMD code.[39] The orbital transitions of selected excited states were characterized using the natural transition orbital (NTO) method.[40]

Following the benchmark calculations of Hadt *et al.*[41] and our previous work,[42] EPR g parameters were computed using the GGA BPW91 functional with the aug-cc-pVTZ-J basis set for the Ti atom,[43] and the IGLO-III basis set for other atoms.[44] The A parameters were computed using the hybrid B3LYP functional with the same basis sets. The aug-cc-pVTZ-J basis sets were taken from the EMSL Basis Set Exchange Web site.[45] All parameters were computed in toluene modelled as a PCM.

Acknowledgements

We thank Dr Jean-Claude Chambron and Dr Yves Canac for stimulating discussions on CH/π interactions and record-breaking ^{31}P NMR shifts in group 4 metal phosphides respectively.

We thank Ms Marie-José Penouilh-Suzette for measuring the HRMS spectra. Financial support from the Centre National de la Recherche Scientifique (CNRS), Agence Nationale de la Recherche and Deutsche Forschungsgemeinschaft (MENOLEP project) and the Conseil Regional de Bourgogne (PARI CDEA program) is gratefully acknowledged.

Keywords: transition metal phosphides • titanium • phosphorus ligands • FLP • DFT

[1] a) K. Issleib and E. Wenschuh, *Chem. Ber.* **1964**, *97*, 715-720; b) K. Issleib and H. Häckert, *Z. Naturforsch. B* **1966**, *21*, 519-521.
[2] For reviews, see : a) E. Hey-Hawkins, *Chem. Rev.* **1994**, *94*, 1661-1717; b) D. W. Stephan, *Angew. Chem. Int. Ed.* **2000**, *39*, 314-329; c) R. Waterman, *Dalton Trans.* **2009**, 18-26; d) L. Rosenberg, *Coord. Chem. Rev.* **2012**, *256*, 606-626.
[3] See refs 1, 2 and a) K. Issleib, G. Wille and F. Krech, *Angew. Chem.* **1972**, *84*, 582-582; b) R. T. Baker, P. J. Krusic, T. H. Tulip, J. C. Calabrese and S. S. Wreford, *J. Am. Chem. Soc.* **1983**, *105*, 6763-6765; c) R. T. Baker, J. F. Whitney and S. S. Wreford, *Organometallics* **1983**, **2**, 1049-1051; d) S. R. Wade, M. G. H. Wallbridge and G. R. Willey, *J. Chem. Soc. Dalton Trans.* **1983**, 2555-2559; e) E. Hey-Hawkins and S. Kurz, *J. Organomet. Chem.* **1994**, *479*, 125-133; f) E. Hey-Hawkins, S. Kurz, J. Sieler and G. Baum, *J. Organomet. Chem.* **1995**, *486*, 229-235; g) C. Frenzel, E. Hey-Hawkins, U. Müller and I. Strenger, *Zeit. Anorg. Allg. Chem.* **1997**, *623*, 277-280; h) S. Xin, H. G. Woo, J. F. Harrod, E. Samuel and A.-M. Lebuis, *J. Am. Chem. Soc.* **1997**, *119*, 5307-5313; i) U. Segerer and E. Hey-Hawkins, *Polyhedron* **1997**, *16*, 2537-2545; j) U. Segerer, S. Blaurock, J. Sieler and E. Hey-Hawkins, *Organometallics* **1999**, *18*, 2838-2842; k) T. Koch, S. Blaurock, F. B. Somoza, A. Voigt, R. Kirmse and E. Hey-Hawkins, *Organometallics* **2000**, *19*, 2556-2563; l) U. Segerer, S. Blaurock, J. Sieler and E. Hey-Hawkins, *J. Organomet. Chem.* **2000**, *608*, 21-26; m) E. Urnezius, S. J. Klippenstein and J. D. Protasiewicz, *Inorg. Chim. Act.* **2000**, *297*, 181-190; n) G. Altenhoff, S. Bredeau, G. Erker, G. Kehr, O. Kataeva and R. Fröhlich, *Organometallics* **2002**, *21*, 4084-4089; o) S. Bredeau, G. Altenhoff, K. Kunz, S. Döring, S. Grimme, G. Kehr and G. Erker, *Organometallics* **2004**, *23*, 1836-1844; p) A. J. Roering, S. N. MacMillan, J. M. Tanski and R. Waterman, *Inorg. Chem.* **2007**, *46*, 6855-6857; q) U. J. Kilgore, H. Fan, M. Pink, E. Urnezius, J. D. Protasiewicz and D. J. Mindiola, *Chem. Commun.* **2009**, 4521-4523; r) A. J. Roering, A. F. Maddox, L. T. Elrod, S. M. Chan, M. B. Ghebreab, K. L. Donovan, J. J. Davidson, R. P. Hughes, T. Shalumova, S. N. MacMillan, J. M. Tanski and R. Waterman, *Organometallics* **2009**, *28*, 573-581; s) A. J. Roering, S. E. Leshinski, S. M. Chan, T. Shalumova, S. N. MacMillan, J. M. Tanski and R. Waterman, *Organometallics* **2010**, 29, 2557-2565; t) M. B. Ghebreab, D. K. Newsham and R. Waterman, *Dalton Trans.* **2011**, *40*, 7683-7685; u) A. J. Roering, L. T. Elrod, J. K. Pagano, S. L. Guillot, S. M. Chan, J. M. Tanski and R. Waterman, *Dalton Trans.* **2013**, *42*, 1159-1167; v) M. B. Ghebreab, C. A. Bange and R. Waterman, *J. Am. Chem. Soc.* **2014**, *136*, 9240-9243; w) A. T. Normand, C. G. Daniliuc, B. Wibbeling, G. Kehr, P. Le Gendre and G. Erker, *Chem. Eur. J.* **2016**, *22*, 4285-4293.
[4] See refs 1, 3a-b, 3d and a) H. Bürger and H.-J. Neese, *Zeit. Anorg. Allg. Chem.* **1969**, *370*, 275-282; b) J. G. Kenworthy, J. Myatt and P. F. Todd, *J. Chem. Soc. Chem. Commun.* **1969**, 263-264; c) J. G. Kenworthy, J. Myatt and P. F. Todd, *J. Chem. Soc. B* **1970**, 791-794; d) J. G. Kenworthy, J. Myatt and M. C. R. Symons, *J. Chem. Soc. A* 1971, 3428-3430; e) H. Bürger and H. J. Neese, *Inorg. Nucl. Chem. Lett.* **1970**, *6*, 299-304; f) H. Köpf and R. Voigtländer, *Chem. Ber.* **1981**, *114*, 2731-2743; g) B. L. Benac and R. A. Jones, *Polyhedron* **1989**, *8*, 1774-1777; h) D. G. Dick and D. W. Stephan, *Organometallics* **1990**, *9*, 1910-1916; i) D. G. Dick and D. W. Stephan, *Can. J. Chem.* **1991**, *69*, 1146-1152; j) D. G. Dick and D. W. Stephan, *Organometallics* **1991**, *10*, 2811-2816; k) R. Payne, J. Hachgenei, G. Fritz and D. Fenske, *Z. Naturforsch. B* **1986**, *41*, 1535-1540; l) D. Fenske, A. Grissinger, E. M. Hey-Hawkins and J. Magull, *Zeit. Anorg. Allg. Chem.* **1991**, *595*, 57-66; m) D. G. Dick, Z. Hou and D. W. Stephan, *Organometallics* **1992**, *11*, 2378-2382; n) J. Ho and D. W. Stephan, *Inorg. Chem.* **1994**, *33*, 4595-4597; o) S. Xin, H. G. Woo, J. F. Harrod, E. Samuel and A.-M. Lebuis, *J. Am. Chem. Soc.* **1997**, *119*, 5307-5313; p) M. Schaffrath, A. Villinger, D. Michalik, U. Rosenthal and A. Schulz, *Organometallics* **2008**, *27*, 1393-1398.

[5] a) R. Shu, L. Hao, J. F. Harrod, H.-G. Woo and E. Samuel, *J. Am. Chem. Soc.* **1998**, *120*, 12988-12989; b) J. D. Masuda, A. J. Hoskin, T. W. Graham, C. Beddie, M. C. Fermin, N. Etkin and D. W. Stephan, *Chem. Eur. J.* **2006**, *12*, 8696-8707; c) A. Perrier, V. Comte, C. Moïse and P. Le Gendre, *Chem. Eur. J.* **2010**, *16*, 64-67.
[6] a) F. Basuli, J. Tomaszewski, J. C. Huffman and D. J. Mindiola, *J. Am. Chem. Soc.* **2003**, *125*, 10170-10171; b) F. Basuli, L. A. Watson, J. C. Huffman and D. J. Mindiola, *Dalton Trans.* **2003**, 4228-4229; c) B. C. Bailey, J. C. Huffman, D. J. Mindiola, W. Weng and O. V. Ozerov, *Organometallics* **2005**, *24*, 1390-1393; d) G. Zhao, F. Basuli, U. J. Kilgore, H. Fan, H. Aneetha, J. C. Huffman, G. Wu and D. J. Mindiola, *J. Am. Chem. Soc.* **2006**, *128*, 13575-13585; e) B. F. Wicker, J. Scott, J. G. Andino, X. Gao, H. Park, M. Pink and D. J. Mindiola, *J. Am. Chem. Soc.* **2010**, *132*, 3691-3693.
[7] a) A. T. Normand, C. G. Daniliuc, B. Wibbeling, G. Kehr, P. Le Gendre and G. Erker, *J. Am. Chem. Soc.* **2015**, *137*, 10796-10808; b) A. T. Normand, C. G. Daniliuc, G. Kehr, P. Le Gendre and G. Erker, *Dalton Trans.* **2016**, *45*, 3711-3714.
[8] F. Silveira, L. M. T. Simplício, Z. N. d. Rocha and J. H. Z. d. Santos, *Appl. Cat. A* **2008**, *344*, 98-106.
[9] This was first observed by Issleib in 1964, see ref 1a. In this case further reduction of $[TiCl_4.(2THF)]$ to Ti(II) gave the intriguing homoleptic complex $[Ti(PCy_2)_2]$.
[10] The phosphinyl radical then recombines to form a diphosphane ($R_2P\text{-}PR_2$).
[11] a) H. Bürger and H.-J. Neese, *Zeit. Anorg. Allg. Chem.* **1969**, *370*, 275-282; b) H. Bürger and H. J. Neese, *Inorg. Nucl. Chem. Lett.* **1970**, *6*, 299-304.
[12] cationic d^0 phosphidotitanocene complexes $[Cp_2TiP(SiMe_3)_2]^+$ and $[Cp_2Ti(PPh_2)(PMe_3)]^+$ have previously been envisaged from a theoretical perspective : a) M. Ehrig, W. Koch and R. Ahlrichs, *Chem. Phys. Lett.* **1991**, *180*, 109-113; b) J. R. Rogers, T. P. S. Wagner and D. S. Marynick, *Inorg. Chem.* **1994**, *33*, 3104-3110.
[13] a) P. Le Gendre, M. Picquet, P. Richard and C. Moïse, *J. Organomet. Chem.* **2002**, *643-644*, 231-236; b) A. T. Normand, P. Richard, C. Balan, C. G. Daniliuc, G. Kehr, G. Erker and P. Le Gendre, *Organometallics* **2015**, *34*, 2000-2011.
[14] The first equivalent of phosphide acts as a sacrificial reductant, generating $R_2P\text{-}PR_2$ as a by-product.
[15] J. W. Lauher and R. Hoffmann, *J. Am. Chem. Soc.* **1976**, *98*, 1729-1742.
[16] as noted elsewhere in the case of amidoziroconcene cations (ref 7a), the lone pair of phosphorus would have to be in the equatorial plane of the bent Cp_2M fragment for π interactions to occur.
[17] B. Cordero, V. Gomez, A. E. Platero-Prats, M. Reves, J. Echeverria, E. Cremades, F. Barragan and S. Alvarez, *Dalton Trans.* **2008**, 2832-2838.
[18] a) M. Nishio, Y. Umezawa, K. Honda, S. Tsuboyama and H. Suezawa, *CrystEngComm* **2009**, *11*, 1757-1788; b) M. Nishio, *CrystEngComm* **2004**, *6*, 130-158.
[19] a) Y. Umezawa and M. Nishio, *Bioorg. Med. Chem.* **1998**, *6*, 493-504; b) X. Xu, B. Pooi, H. Hirao and S. H. Hong, *Angew. Chem. Int. Ed.* **2014**, *53*, 1283-1287.
[20] In order to circumvent hydrolysis by residual water, measurements were conducted on 10^{-2}M solutions of the complexes in 0.1mm cells
[21] a) D. Escudero, A. D. Laurent and D. Jacquemin *Time-Dependent Density Functional Theory: A Tool to Explore Excited States*, *in* Handbook of Computational Chemistry, (Ed. J. Leszczynski), Springer, Dordrecht, **2015**; b) Z. Li and W. Liu, *J. Chem. Theory Comput.* **2016**, *12*, 2517-2527.
[22] a) S. L. Borkowsky, N. C. Baenziger and R. F. Jordan, *Organometallics* **1993**, *12*, 486-495; b) W. Ahlers, B. Temme, G. Erker, R. Fröhlich and F. Zippel, *Organometallics* **1997**, *16*, 1440-1444.
[23] We have previously used phi as an indicator of π interactions between Zr and N or P in zirconocene complexes, see ref 7a.
[24] It is interesting to note that a clear π interaction was found by Alhrichs in the Ti(III) $[Cp_2TiP(SiMe_3)_2]$ complex (ref 12a). The Ti-P π interaction in this complex is possible because the metallocene fragment is supported only by the phosphide ligand : therefore, the single electron on titanium and the pπ electrons on phosphorus occupy orthogonal orbitals This is no longer possible in complexes 2 in which the titanium atom is tetracoordinated: all d orbitals are involved in bonds and the single electron is bound to interact with the lone pair of the phosphido ligand. This leads to a bent geometry, a classical situation in phosphido ligand chemistry (see ref 2d).
[25] ^{1}H NMR signals were assigned unambiguously through ^{1}H-^{13}C correlation experiments, i.e. HSQC and HMBC. Also, the ^{31}P spectrum of **3b** shows that the hydrogens on C11 couple with P1, not P2. See supporting information.
[26] O. Kühl *The Range of Chemical Shifts, Coupling Constants, and What Influences Each*, *in* Phosphorus-31 NMR Spectroscopy: A Concise Introduction for the Synthetic Organic and Organometallic Chemist, (Ed. O. Kühl), Springer Berlin Heidelberg, Berlin, Heidelberg, **2008**, pp. 7-23.
[27] Differences between $^3J_{PH}$ coupling constants in $CpCH_2CH_2PR_2$ ligands have been observed before, see for example Janssen, K.; Butenschon, H., *New J. Chem.* **2011**, *35*, 2287-2298.
[28] The exact chemical shift could not be ascertained due to multiple overlaps in the ^{1}H NMR spectrum of **3d**.
[29] S. Halbert, C. Copéret, C. Raynaud and O. Eisenstein, *J. Am. Chem. Soc.* **2016**, *138*, 2261-2272.
[30] We also observed small intensity (ε = 2210-3220 $cm^{-1}.M^{-1}$) shouldering bands in the UV region (**3b** -> 348 nm; **3c** -> 342 nm; **3d** -> 346 nm), although we were unable to assign them through DFT calculations.
[31] although the absence of $(PCy_2)_2$ is surprising in the case of **3f**, it could just be that the presence of PCy_2H in the reaction mixture prevents the phosphinyl radical from dimerizing, instead promoting other termination pathways, *e.g.* H abstraction from the solvent.
[32] Complex **E** was characterized in C_6D_5Br at 299 K, see ref 7a.
[33] a) J. Y. Lan and G. B. Schuster, *J. Am. Chem. Soc.* **1985**, *107*, 6710-6711; b) S. T. Murphy, C. Zou, J. B. Miers, R. M. Ballew, D. D. Dlott and G. B. Schuster, *J. Phys. Chem.* **1993**, *97*, 13152-13157; c) O. Grinevich, P. Serguievski, A. M. Sarker, W. Zhang, A. Mejiritski and D. C. Neckers, *Macromolecules* **1999**, *32*, 328-330.
[34] Y. Hasegawa, G. Kehr, S. Ehrlich, S. Grimme, C. G. Daniliuc and G. Erker, *Chem. Sci.* **2014**, *5*, 797-803.
[35] A. T. Normand, C. G. Daniliuc, B. Wibbeling, G. Kehr, P. Le Gendre and G. Erker, *Chem. Eur. J.* **2016**, *22*, 4285-4293.
[36] Gaussian 09. Revision D. 01. Frisch. M. J. et al. Gaussian. Inc., Wallingford CT, 2009
[37] a) F. Weigend, *Phys. Chem. Chem. Phys.* **2006**, *8*, 1057-1065; b) F. Weigend and R. Ahlrichs, *Phys. Chem. Chem. Phys.* **2005**, *7*, 3297-3305.
[38] a) B. Mennucci, J. Tomasi, R. Cammi, J. R. Cheeseman, M. J. Frisch, F. J. Devlin, S. Gabriel and P. J. Stephens, *J. Phys. Chem. A* **2002**, *106*, 6102-6113; b) J. Tomasi, B. Mennucci and R. Cammi, *Chem. Rev.* **2005**, *105*, 2999-3093.
[39] W. Humphrey, A. Dalke and K. Schulten, *J. of Mol. Graph.* **1996**, *14*, 33-38.
[40] R. L. Martin, *J. Chem. Phys.* **2003**, *118*, 4775-4777.
[41] R. G. Hadt, V. N. Nemykin, J. G. Olsen and P. Basu, *Phys. Chem. Chem. Phys.* **2009**, *11*, 10377-10384.
[42] E. Lerayer, P. Renaut, S. Brandès, H. Cattey, P. Fleurat-Lessard, G. Bouhadir, D. Bourissou and J.-C. Hierso, *Inorg. Chem.* **2017**, *56*, 1966-1973.
[43] a) L. Goerigk and S. Grimme, *J. Chem. Theory Comput.* **2011**, *7*, 291-309; b) N. B. Balabanov and K. A. Peterson, *J. Chem. Phys.* **2005**, *123*, 064107.
[44] W. Kutzelnigg, U. Fleischer and M. Schindler, (Berlin, Heidelberg) **1991**, pp. 165-262.
[45] https://bse.pnl.gov/bse/portal, accessed 04/05/2016.